New manifestation of the dispersion relation: Breakup Threshold Anomaly.

M. S. Hussein[1], P. R. S. Gomes[2], J. Lubian[2] and L. C. Chamon[1].
[1]*Instituto de Física da Universidade de São Paulo,*
Caixa Postal 66318, 05315-970, São Paulo, SP, Brazil.
[2]*Instituto de Física, Universidade Federal Fluminense,*
Av. Litoranea s/n, Gragoatá, Niterói, RJ, Brazil, 24210-340.
(Dated: February 4, 2008)

It is pointed out that the usual threshold anomaly, found operative in the energy behavior of the imaginary and real parts of the optical potential representing the elastic scattering of tightly bound nuclei at near- and below-barrier energies, suffers a drastic qualitative change in the case of the elastic scattering of weakly bound nuclei. Owing to the strong coupling to the breakup channel even at sub-barrier energies, the imaginary potential strength seems to increase as the energy is lowered down to below the natural, barrier, threshold, accompanied by a decrease in the real potential strength. This feature is consistent with the dispersion relation. The system ^{6}Li + ^{208}Pb is analyzed to illustrate this new phenomenon.

PACS numbers: 25.70.Bc,25.70.Mn

The, by now, well known Threshold Anomaly (TA), seen in the behavior of the real and imaginary parts of the optical potential as a function of decreasing energy in the elastic scattering of tightly bound nuclei at near-barrier energies, has been discussed and reviewed by several authors [1, 2, 3]. The phenomenon is a direct consequence of the dispersion relation which quantifies the concept of causality in scattering: no scattered wave emerges before the incident wave reaches the target. Recently, the TA has been looked for in the case of the elastic scattering of weakly bound stable and radioactive nuclei [4, 5, 6, 7, 8, 9, 10]. Careful analyses of the data show that what happens in these systems is a new manifestation of the dispersion relation unique for breakup coupling dynamic polarization potential. Because the coupling to the breakup in these systems continues to be important even at energies below the barrier, the "threshold" ceases to be the barrier itself. Thus, the imaginary part of the potential could increase at lower energies and, as the dispersion relation dictates, the real part of the dynamic potential would show a decrease, implying an overall decrease in the real part of the optical potential that fits the elastic scattering. This is indeed what is found [4, 5, 6, 7, 8, 9, 10]. The purpose of this paper is to give an account of this phenomenon, which we coin as the Breakup Threshold Anomaly (BTA).

We analyze a system involving the ^{6}Li weakly bound nucleus: ^{6}Li + ^{208}Pb. We have re-analyzed the elastic scattering angular distribution data [6] using the São Paulo (SP) optical potential. The choice of this potential is due to the fact that it has been successfully used in the study of several systems [11]. The conclusions obtained here, however, do not depend on this particular choice of potential. The SP interaction [11, 12, 13, 14, 15] is based on the double folding potential with account to exchange through an effective energy dependence:

$$V_{SP}(R,E) = (1 + i\ 0.78)\, F(R,E), \qquad (1)$$

where $F(R,E)$ is the double folding potential whose energy dependence results from the local equivalence of the otherwise non-local interaction [15, 16]. This energy dependence is not dispersive. The $F(R,E)$ term is given by:

$$F(R,E) = V_F(R)\ e^{-4\mathrm{v}^2/c^2}\ , \qquad (2)$$

where c is the speed of light and v is the local relative velocity between the two nuclei,

$$\mathrm{v}^2(R,E) = \frac{2}{\mu}\ [E - V_C(R) - V_N(R,E)]\ , \qquad (3)$$

where V_N is the real part of the nuclear interaction and V_C is the Coulomb potential. The folding potential depends on the matter densities of the nuclei involved in the collision:

$$V_F(R) = \int \rho_1(\vec{r}_1)\ \rho_2(\vec{r}_2)\ V_0\ \delta(\vec{R} - \vec{r_1} + \vec{r_2})\ d\vec{r_1}, \qquad (4)$$

with $V_0 = -456$ MeV fm^3. The use of the matter densities and delta function in Eq. (4) corresponds to the zero-range approach for the folding potential, which is equivalent [14] to the more usual procedure of using the M3Y effective nucleon-nucleon interaction with the nucleon densities of the nuclei (instead of the matter densities). With the aim of providing a parameter free description of the interaction, we proposed [14] an extensive systematics of nuclear densities. For this purpose, we adopted the two-parameter Fermi (2pF) distribution to describe the densities. The radii of the 2pF distributions are well represented by

$$R_0 = 1.31A^{1/3} - 0.84 \text{ fm}, \qquad (5)$$

where A is the number of nucleons of the nucleus. The values obtained for the matter diffuseness of the distributions are very similar throughout the periodic table and present small deviations around the average value $a = 0.56$ fm. In this work, we use the São Paulo potential in the context of this systematics by assuming the

average diffuseness value and Eq. (5) to determine the radii of the density distributions.

In the present analysis, we have assumed for the optical potential a normalized version of the SP potential:

$$V_{SP}(R,E) = [N_R(E) + iN_I(E)]\, F(R,E). \qquad (6)$$

The coefficients $N_R(E)$ and $N_I(E)$ are energy dependent normalization factors that take into account the effects of the dynamic polarization potentials (DPP) arising from direct channel couplings. It is worth mentioning here that all DPP´s are dispersive with their real and imaginary parts being connected through a dispersion relation. One important exception to this is the elastic transfer DPP [17].

From the properties of the Green function, that enters in the definition of the DPP, one can immediately derive the dispersion relation between $N_R(E)$ and $N_I(E)$, represented by:

$$N_R(E) = N_{R0} + \Delta N_R(E), \qquad (7)$$

$$\Delta N_R(E) = \frac{P}{\pi}\int \frac{N_I(E')}{E'-E}dE', \qquad (8)$$

and its subtracted form

$$\Delta N_R(E) = \Delta N_R(E_s) + (E-E_s)\frac{P}{\pi}\int \frac{N_I(E')}{(E'-E_s)(E'-E)}dE', \qquad (9)$$

where E_s is some high enough energy at which information about both N_I and ΔN_R are known [2]. These equations are the analog of the Kramer-Kronig dispersion relation in optics, from general principle of causality, already mentioned above.

The dashed lines in figure 1 represent predictions, for the elastic scattering of ^{6}Li + ^{208}Pb, obtained with the energy-independent standard values $N_R = 1$ and $N_I = 0.78$, while the solid lines correspond to the results obtained with the best fit N_R and N_I values. A comparison between these dashed and solid lines shows that the data fit is quite sensitive to the N_R and N_I values.

Just to illustrate the dispersion relation, we have assumed a schematic description for N_I

$$N_I = 0 \text{ for } E \le E_1, \qquad (10)$$

$$N_I = a(E-E_1) \text{ for } E_1 \le E \le E_2, \qquad (11)$$

$$N_I = a(E_2-E_1) + b(E-E_2) \text{ for } E_2 \le E \le E_3, \qquad (12)$$

$$N_I = a(E_2-E_1) + b(E_3-E_2) = N_{I\infty} \text{ for } E \ge E_3. \qquad (13)$$

Within this assumption, and owing to the constancy of N_I at $E > E_3$, the subtracted dispersion relation, Eq. (9), gives the same result as the non-subtracted one, Eq. (8). Using Eq. (8) and Eqs. (10-13), one obtains an analytical expression for ΔN_R [2, 3]

$$\begin{aligned}\Delta N_R(E) \;=\; & a(E_2-E_1)\,[\epsilon_1 ln|\epsilon_1| - \epsilon_2 ln|\epsilon_2|] \\ & + [b(E_3-E_2) - a(E_2-E_1)] \\ & \times [\epsilon'_2 ln|\epsilon'_2| - \epsilon'_3 ln|\epsilon'_3|]\,,\end{aligned} \qquad (14)$$

with $\epsilon_i = (E-E_i)/(E_2-E_1)$ and $\epsilon'_i = (E-E_i)/(E_3-E_2)$. By using Eqs. (7) and (14), one can find $N_R(E)$ in an independent way of the reference energy E_S.

In figure 2 we present the best fit $N_R(E)$ and $N_I(E)$ values. The uncertainties of these quantities have been obtained by considering the range where $N_R(E)$ and $N_I(E)$ could vary which would result in an increase of the chi-square value by unity relative to the corresponding minimum value. The lines in figure 2 represent possible behaviors of N_R and N_I that are compatible with the dispersion relation. A striking difference in the energy dependence of these normalization coefficients from the usual energy dependence of tightly bound systems is clearly seen. As the energy is lowered below the barrier $N_R(E)$ decreases, while $N_I(E)$ increases. This implies an effective reduction of the nuclear attraction leading to an increase in the barrier height.

A further evidence of the consistency of our analyses are the values obtained for N_{R0} and $N_{I\infty}$. As the SP potential, equation (1), has been successful in describing the elastic scattering for a large number of different systems at energies above the barrier [11], one should expect that both N_{R0} and $N_{I\infty}$ to be close to unity. Of course, the values for N_{R0} and $N_{I\infty}$ found in the present work are not identical to the standard (from high energies) N_R=1 and N_I=0.78. However, these standard values in fact represent mean values obtained from data analyses of several systems [11] and one can expect variations around the average values for particular systems. Indeed, structure effects on the nuclear densities involved in the folding calculations may affect N_R while different degrees of absorption from particular reaction channels could affect N_I. An inspection of Fig. 2 shows that $N_{R0} \approx 1$ and $N_{I\infty} \approx 1$ have been found in the present work.

As already commented, the solid lines in Fig. 2 represent behaviors of N_R and N_I compatibles with the dispersion relation. In fact, different behaviors, that also could follow the "data", can be found. Therefore, clearly our findings are mainly based on the N_R and N_I "data" themselves. The detected difference between the normal and weakly-bound systems is mostly based on the results from the corresponding lowest energies (see Fig. 2). Even so, we consider that significant evidence for the proposed BTA has been obtained, because the data fits for these low energies are quite sensitive to N_R and N_I, as illustrated by the dashed and solid lines in Fig. 1. We mention that similar behavior of the increasing of the imaginary potential as the energy decreases towards the barrier was already observed earlier for the same system [9] using different data analysis procedures and also for the following other systems: ^{9}Be + ^{209}Bi [4, 5], ^{6}Li

+ ^{28}Si, ^{58}Ni, ^{122}Sn, ^{138}Ba [7, 9] and ^{9}Be + ^{64}Zn [10], although in these previous works there is no attempt to explain the behavior of the energy dependence of the real and imaginary parts of the optical potential as the BTA phenomenon.

Traditionally, the threshold anomaly is formally displayed in terms of complex renormalization factors of the double-folding potential, as we have done in the present work. This assumption, which corresponds to assuming that the radial dependence of the optical potential is the same as the bare one, is well established for normal tightly bound stable nucleus systems. The situation is more complicated in the case of weakly bound nuclei, where the effect of the couplings give rise to a polarization potential with different radial shape. In particular, an important role is played by the tail of the polarization which is much longer than that of the folding potential [18]. Nevertheless, our simple approach of considering renormalization factors has provided good fits for all angular distributions analyzed in the present work

In conclusion, we have found some evidence of differences in the energy-dependence of the optical potential for tightly and weakly bound nuclei. The Break-up Threshold Anomaly implies an increase of the imaginary part and a decrease of the real part of the optical potential that fits the elastic scattering at low energies. Our findings have mostly been based on the results obtained from elastic scattering data analyses for the lowest energies of one system, and also on earlier data analyses for other similar systems [4, 5, 6, 7, 8, 9, 10]. Clearly more work is required to further improve our understanding of the BTA.

Acknowledgments

This work was partially supported by Financiadora de Estudos e Projetos (FINEP), Fundação de Amparo à Pesquisa do Estado de São Paulo (FAPESP), Fundação de Amparo à Pesquisa do Estado do Rio de Janeiro (FAPERJ), Instituto de Milênio de Informação Quântica (MCT), and Conselho Nacional de Desenvolvimento Científico e Tecnológico (CNPq).

[1] M. A. Nagarajan, C. C. Mahaux and G. R. Satchler, Phys. Rev. Lett. **54**, 1136 (1985).
[2] G. R. Satchler, Phys. Rep. **199**, 147 (1991).
[3] M. E. Brandan and G. R. Satchler, Phys. Rep. **285**, 143 (1997).
[4] C. Signorini, Europ. Phys. Journal **A13**, 129 (2002).
[5] C. Signorini et al., Phys. Rev. **C61** 061603(R) (2000).
[6] N. Keeley, S. J. Bennett, N. M. Clarke, B. R. Fulton, G. Tungate, P. V. Drumm, M. A. Nagarajan, J. S. Lilley, Nucl. Phys. **A571**, 326 (1994).
[7] A. Pakou et al., Phys. Rev. **C69**, 054602 (2004).
[8] I. Martel, J. Gomez-Camacho, K. Rusek, G. Tungate, Nucl. Phys. **A605**, 417 (1996).
[9] A. M. M. Maciel et al., Phys. Rev. **C59**, 2103 (1999).
[10] S.B. Moraes et al., Phys. Rev. **C61**, 064608, (2000).
[11] M. A. G. Alvarez et al., Nucl. Phys. **A723**, 93 (2003).
[12] L. C. Chamon, D. Pereira, M. S. Hussein, M. A. Candido Ribeiro and D. Galetti, Phys. Rev. Lett. **79**, 5218 (1997).
[13] L. C. Chamon, D. Pereira and M. S. Hussein, Phys. Rev. **C58**, 576 (1998).
[14] L. C. Chamon et al., Phys. Rev. **C66**, 014610 (2002).
[15] M. A. Candido Ribeiro, L. C. Chamon, D. Pereira, M. S. Hussein and D. Galetti, Phys. Rev. Lett. **78**, 3270 (1997).
[16] D. T. Khoa, G. R. Satchler and W. von Oertzen, Phys. Rev. **C56**, 954 (1997).
[17] A. Lepine-Szily, M. S. Hussein, R. Lichtenthaler, J. Cseh and G. Levai, Phys. Rev. Lett. **82**, 3972 (1999).
[18] R. S. Mackintosh and N. Keeley, Phys. Rev. **C70**, 024604 (2004).

FIG. 1: Elastic scattering angular distributions for the ^{6}Li + ^{208}Pb system (data from [6]). The solid lines represent the optical model results obtained considering the best fit N_R and N_I parameters. The dashed lines correspond to the SP potential with the standard $N_R = 1$ and $N_I = 0.78$ values.

FIG. 2: Energy dependence of the normalization factors N_R and N_I of the SP potential for the ^{6}Li + ^{208}Pb system. The lines represent possible behaviors of N_R and N_I that are compatible with the dispersion relation.

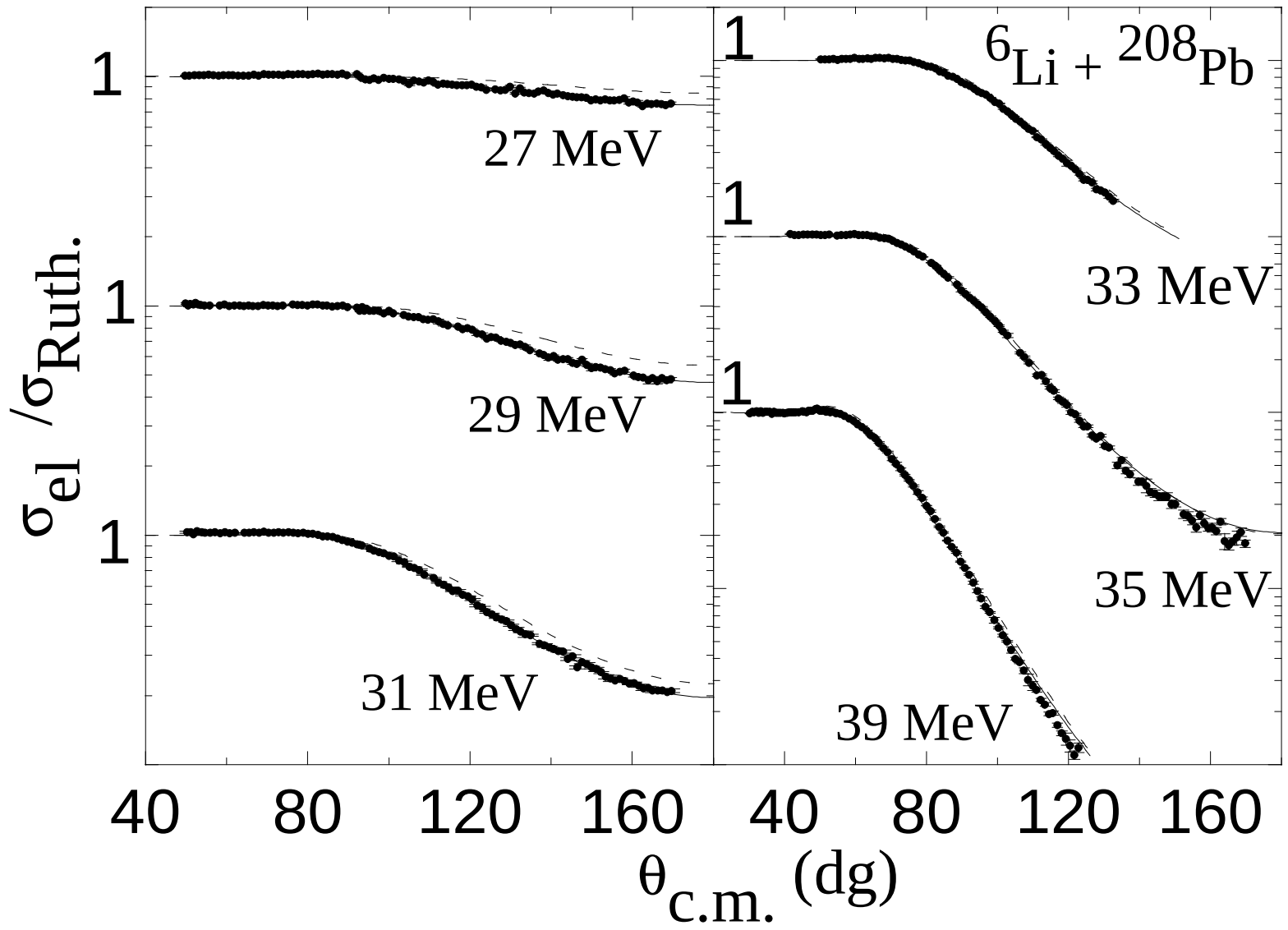
^{6}Li + ^{208}Pb
27 MeV
29 MeV
31 MeV
33 MeV
35 MeV
39 MeV
1
σ_{el} /$\sigma_{Ruth.}$
40
80
120
160
$\theta_{c.m.}$ (dg)

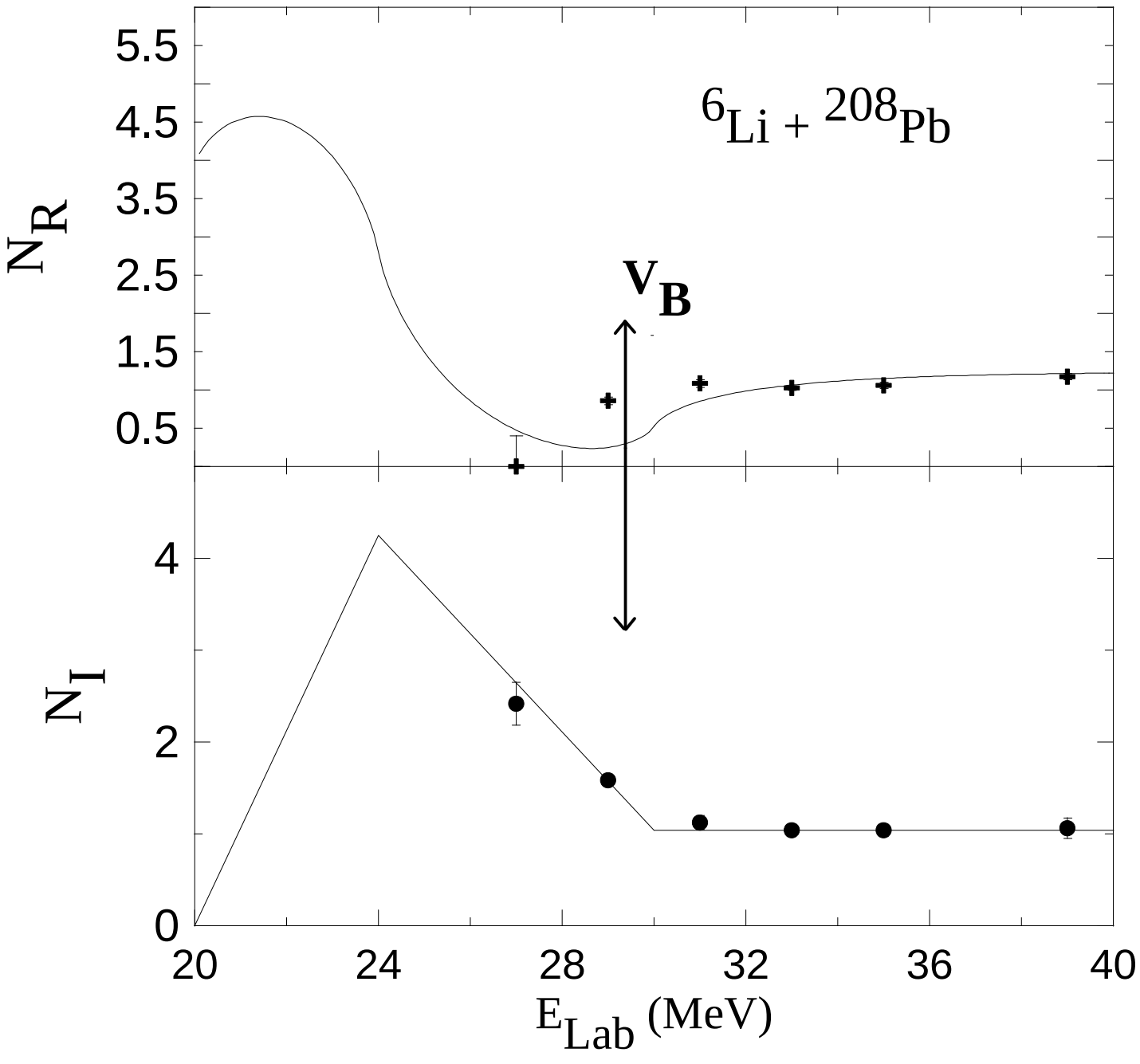
$^{6}Li + ^{208}Pb$
V_B
N_R
N_I
5.5
4.5
3.5
2.5
1.5
0.5
4
2
0
20
24
28
32
36
40
E_{Lab} (MeV)